Wilmeth, D.T., et al., 2022, Evidence for benthic oxygen production in Neoarchean lacustrine stromatolites: Geology, v. 50, https://doi.org/10.1130/G49894.1

Supplementary Text

Geochemical analyses

Laser ablation high-resolution inductively coupled plasma mass spectrometry was performed at the Institut Universitaire Européen de la Mer, Plouzané, France on a on a Thermo ElementXR high-resolution inductively coupled plasma mass spectrometer (HR-ICP-MS) operating at low resolution coupled to a Coherent Inc. GeoLas 193 nm Excimer laser ablation system. Spot sizes were 120 µm at 20 J with a shot frequency of 10 Hz. Calibration was performed using the glass standards BIR-G and BCR-G and data were treated with Fe as an internal standard using the Matlab package SILLS (Guillong et al., 2008). Electron microprobe analysis was performed on a Cameca SX100 at IFREMER, Plouzané, France, operating at 15kV and 20 nA with a spot size of 5 µm. Raman analyses were performed on a Horiba XploRa+ micro-Raman spectrometer and a Horiba XGT-7200 micro-XRF analyzer at the Natural History Museum of Los Angeles County, California, and an Olympus FV1000 confocal laser scanning microscope coupled with a Renishaw InVia Raman Spectrometer at the Institut de Physique du Globe de Paris, France.

Detrital vs. authigenic oxides in Hartbeesfontein stromatolites

As noted in Wilmeth et al., 2019, detrital volcaniclastic sediments within Hartbeesfontein stromatolite laminae contain finely disseminated yellow oxyhydroxides less than 5 µm in diameter with non-metallic luster (Fig. S2). The oxyhydroxides' size distribution, optical properties, and close association with detrital material contrast with larger, metallic laminar oxides, which occur throughout stromatolite laminae regardless of detrital material (Fig. 1G-I). EMPA analysis of detrital material within stromatolite laminae yielded an Al-rich signal distinct from laminar oxides (Table S1). This study therefore considers disseminated oxyhydroxides and laminar oxides as two distinct phases.

Rare earth element (REE) patterns

Along with the nineteen REE spectra and Ce anomalies shown in Fig. 5, four additional LA-ICP-MS data points from laminar oxides are included in Table S2. A Ce anomaly could not be calculated from N1SC1-1f 4 due to a lack of Nd. Two laser shots (N1-SC1-1e 31 and 35) contain REE datasets which differ significantly from other points. These locations are more enriched in LREE than other data points by orders of magnitude. For example, La concentrations in N1-SC1-1e 31 and 35 are 5524 and 6673 µg/g respectively, compared to the next highest value of 518 in N1SC1-1f 2. The samples are also highly enriched in Pb (1482 and 4642 µg/g, respectively) compared with other samples, which typically fall below 600 µg/g Pb. While both locations have negative Ce anomalies, elevated LREE concentrations compared with other laser shots are indicative of secondary enrichment (Bonnand et al., 2020), which could also potentially explain elevated Pb concentrations. One final point (N1-SC1-1e 32) is slightly less enriched in LREE, but also contains abundant Pb (2003 µg/g) and is therefore also excluded from consideration in Fig. 5 and discussion of Ce anomalies.

Figure S1: Locations of LA-ICP-MS laser spots in Figure 2 and Table S2
Diamonds represent fenestral oxides, circles represent laminar oxides, triangles represent external weathering rinds. Numbers refer to samples listed in Table S2.

Figure S2: Detrital material within Hartbeesfontein stromatolites
Petrographic images of detrital material in Hartbeesfontein stromatolite laminae, as opposed to fenestral oxides (Fig. 2) and isolated, dark laminar oxides ~20 microns in diameter (Fig. 3). A-C: Cross-sections of stromatolite mesostructure, with arrows highlighting patches of detrital material within laminae. B and C were taken from the same location using transmitted and reflected light, respectively. Note how detrital patches frequently contain yellow iron oxy-hydroxide minerals. D-E: An individual patch of detrital material within a stromatolite layer. D and E were taken from the same location using reflected and transmitted light, respectively. F: Laminar oxides within a Hartbeesfontein stromatolite for comparison with detrital material, taken using transmitted light. for comparison. Note the contrast between the isolated, dark laminar oxides and the diffuse yellow detrital minerals. G, H: Petrographic cross-section of an Archean volcaniclastic tuff deposit in the Hartbeesfontein Basin. Note the similarities between the tuff petrography and the detrital material in D and E, composed of long, needle-like silicate minerals with interstitial yellow oxy-hydroxides.

Figure S3: Raman spectra from Hartbeesfontein oxides. A: Fenestral oxides, potential goethite signature (spectrum from Wilmeth et al., 2019). B-D: Individual laminar oxides analyzed in this study. Circles note locations of Raman spectral acquisition

Fig. S1

N1SC1-1e

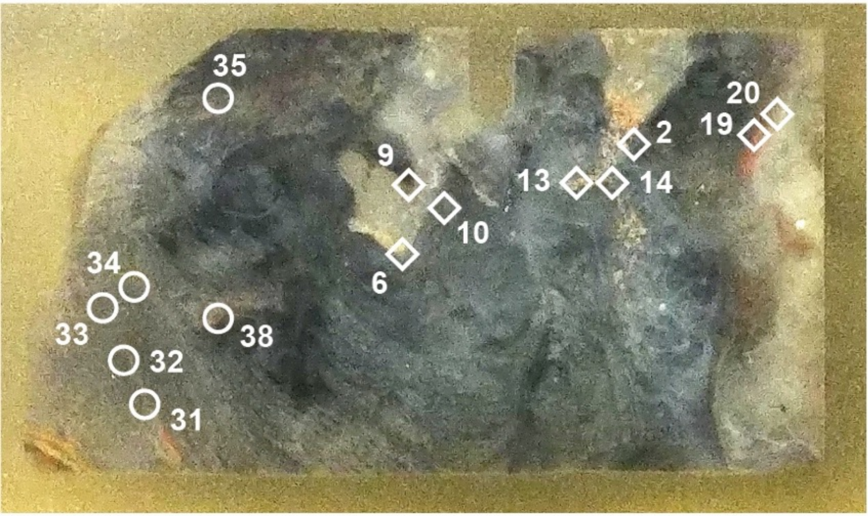

N1SC1-1f

1 cm

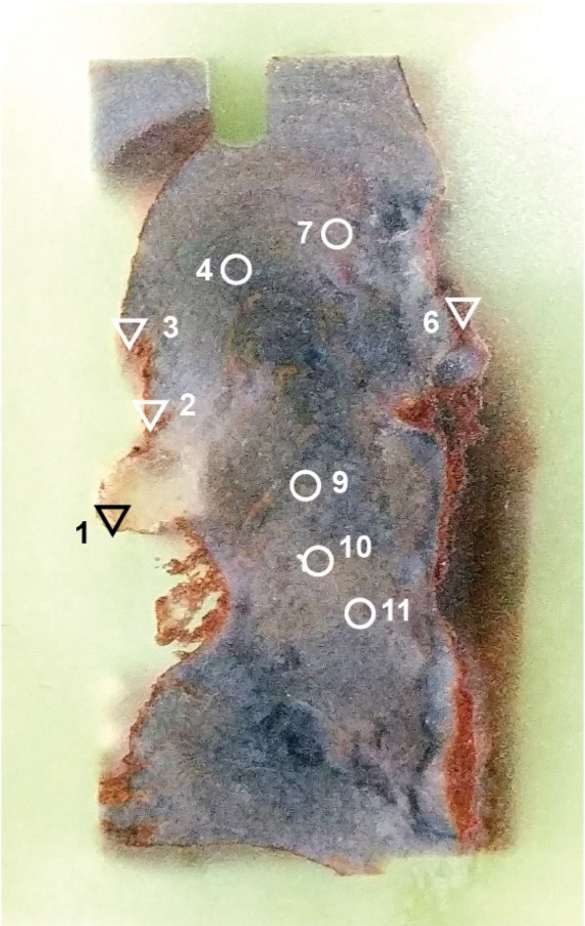

Fig. S2

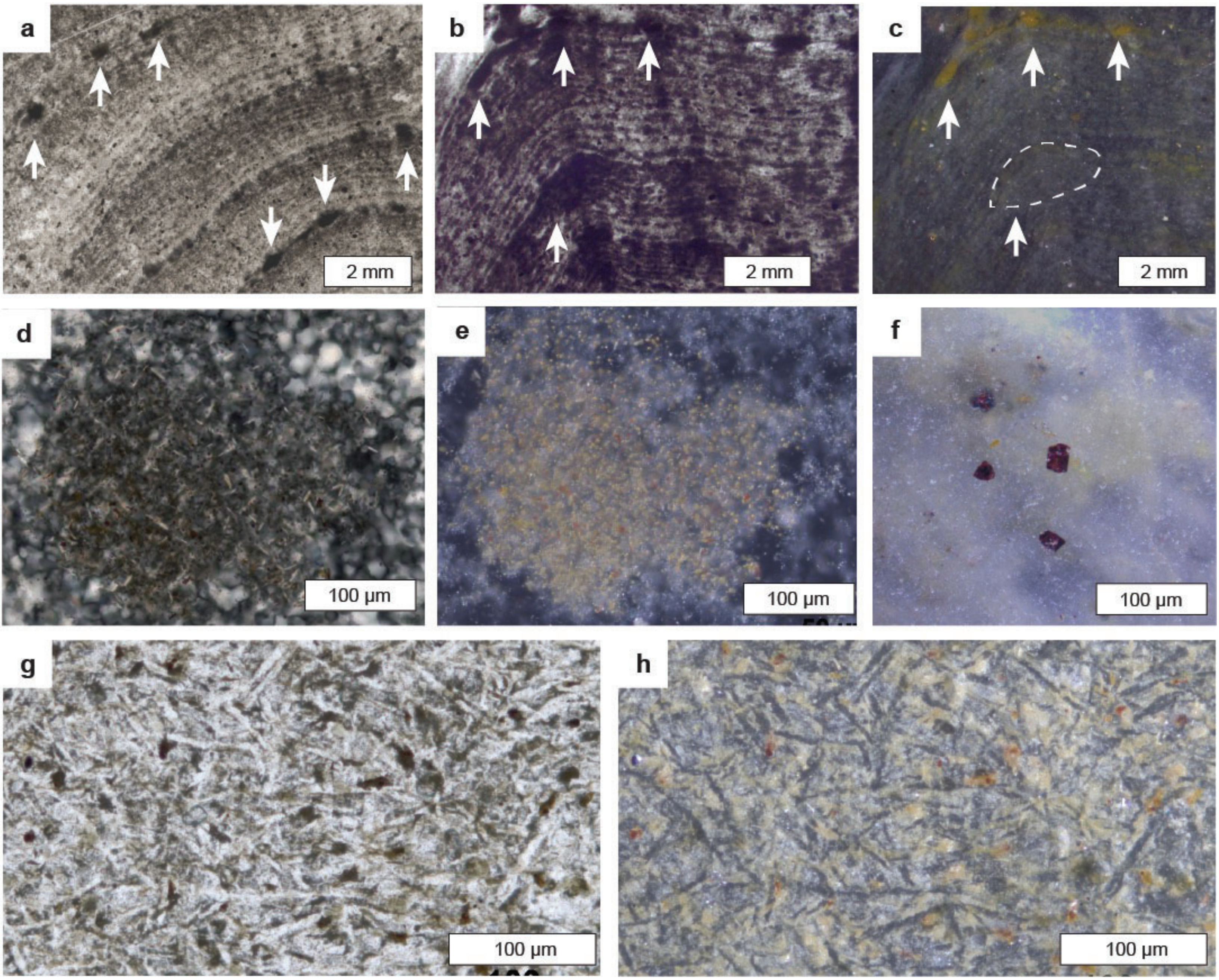

Fig. S3

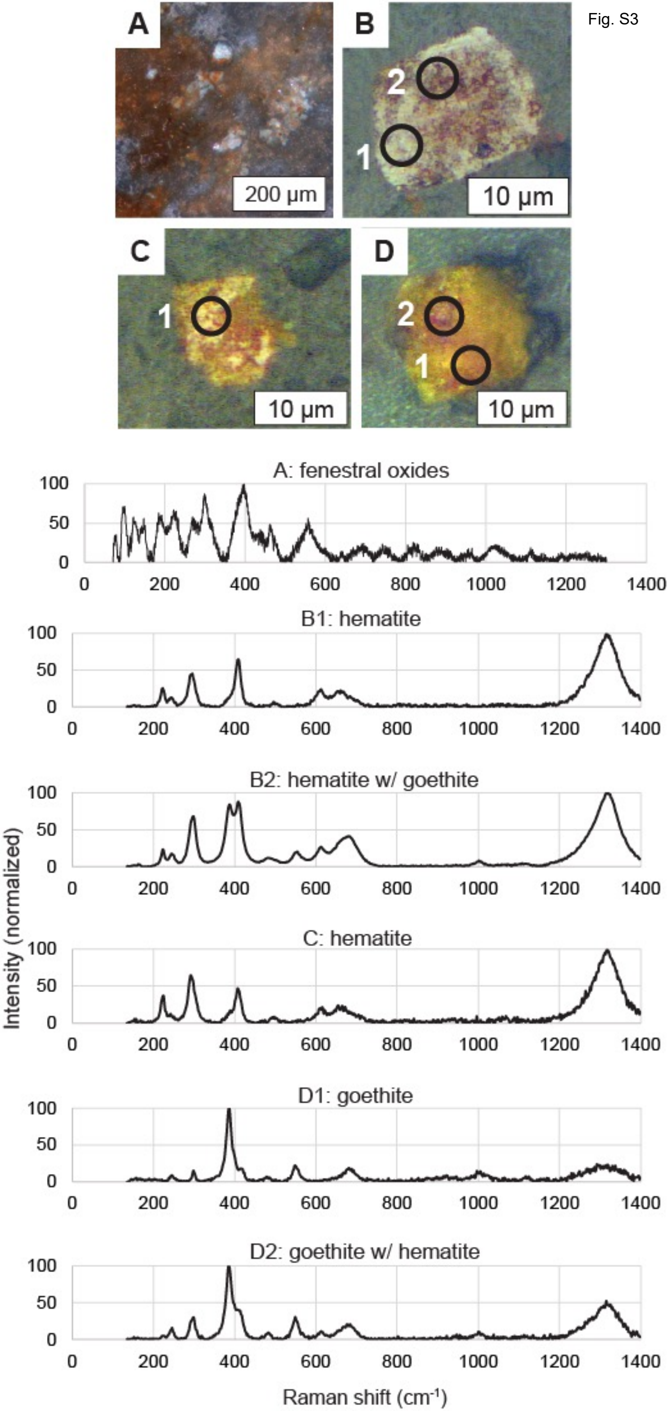
A
200 µm
B
2
1
10 µm
C
1
10 µm
D
2
1
10 µm
A: fenestral oxides
B1: hematite
B2: hematite w/ goethite
C: hematite
D1: goethite
D2: goethite w/ hematite
Intensity (normalized)
Raman shift (cm-1)
0
50
100
0
200
400
600
800
1000
1200
1400